Bimodal and Gaussian Ising spin glasses in dimension two

P. H. Lundow, Ian Campbell

The bimodal and Gaussian Ising Spin Glasses in dimension two revisited

P. H. Lundow[1] and I. A. Campbell[2]

[1] *Department of Mathematics and Mathematical Statistics, Umeå University, SE-901 87, Sweden*
[2] *Laboratoire Charles Coulomb (L2C), UMR 5221 CNRS-Université de Montpellier, Montpellier, F-France.*

A new analysis is given of numerical simulation data on the archetype square lattice Ising Spin Glasses (ISG) with a bimodal ($\pm J$) and Gaussian interaction distributions. It is well established that the ordering temperature of both models is zero. The Gaussian has a non-degenerate ground state so exponent $\eta \equiv 0$ and it has a continuous distribution of energy levels. For the bimodal model, above a size-dependent cross-over temperature $T^*(L)$ there is a regime of effectively continuous energy levels; below $T^*(L)$ there is a distinct regime dominated by the highly degenerate ground state plus an energy gap to the excited states. $T^*(L)$ tends to zero at very large L leaving only the effectively continuous regime in the thermodynamic limit. We show that in this regime the critical exponent η is not zero, so the effectively continuous regime 2D bimodal ISG is not in the same universality class as the 2D Gaussian ISG. The simulation data on both models are analyzed using a scaling variable $\tau = T^2/(1+T^2)$ suitable for zero temperature transition ISGs, together with appropriate scaling expressions. Accurate simulation estimates can be obtained for the temperature dependence of the thermodynamic limit reduced susceptibility $\chi(\tau)$ and second moment correlation length $\xi(\tau)$ over the entire range of temperature from zero to infinity. The Gaussian critical exponent from the simulations $\nu = 3.5(1)$ is in full agreement with the well established value from the literature. The bimodal exponent from the thermodynamic limit regime analysis is $\nu = 4.2(1)$, once again different from the Gaussian value.

PACS numbers: 75.50.Lk, 75.40.Mg, 05.50.+q

I. INTRODUCTION

The canonical Edwards-Anderson (EA) model Ising Spin Glasses (ISGs) in dimension $d = 2$ have been the subject of very many numerical studies. There is now consensus supported by analytic arguments that the two archetype models, the ISGs on square lattices with near neighbor interactions having distributions which are either Gaussian or Bimodal ($\pm J$), have zero temperature transitions [1, 2]. For the Gaussian case, where the interaction distribution is continuous and the ground state is unique, there is now also general consensus concerning the low temperature thermodynamic limit (ThL) behavior and exponents. In the bimodal case there is an "effectively continuous energy level distribution" regime coming down from high temperatures and ending with a crossover at a size dependent temperature $T^*(L)$ to a ground state dominated regime [3]. Interpretations differ considerably concerning the critical exponents for the bimodal interaction case. We will give a new analysis of accurate numerical Monte Carlo data up to size $L = 128$ on the bimodal system in the ThL and up to $L = 64$ on the Gaussian system. We use the temperature T or the inverse temperature β when it is convenient.

We first discuss discuss the specific heat using data from the simulations and independent data down to low temperatures and large sizes from Refs. [4] and [5]. Then we analyse the simulation data for other observables to obtain reliable and accurate estimates for the critical exponents of the ThL regime, using both the conventional scaling variable T and a novel scaling variable compatible with the generic scaling approach for ISGs introduced in [6], adapted to a situation where $T_c = 0$. We find that the Gaussian model and the bimodal model in the ThL are not in the same universality class.

The 2D Gaussian model is relatively clear-cut. Because $T_c = 0$ and the interaction distribution is continuous, there is a unique ground state (for each sample) and the low temperature excitation distribution has no gap. The fact that the ground state is unique necessarily implies that for all L, as $T \to 0$, $\xi(T, L) \to \infty$ and the reduced susceptibility $\chi(T, L) \to L^2$. With T chosen as the critical scaling variable, the standard thermodynamic limit low temperature critical expressions are $\xi(T) \sim T^{-\nu}$ and $\chi(T) \sim T^{-\gamma} = T^{-2\nu}$ because the critical exponent η is strictly zero. The critical behavior of both the observables at low temperature is governed by the single exponent ν, which is related to the stiffness exponent through $\theta = -1/\nu$. Accurate zero temperature domain wall stiffness measurements to large sizes [1, 7–11] show that $\theta = -0.285(2)$, i.e. $\nu = 3.50(3)$.

In the 2D bimodal case the situation is complicated by two factors. First, the ground state is not unique but is massively degenerate; the zero-temperature entropy per spin is $S_0 = 0.078(5)k_B$ [11–13]. Secondly, the distribution of excited state energy levels is not continuous but increases by steps of $4J$; in particular there is an energy gap $4J$ between the ground state and the first excited state. One can write [4] the "naïve" leading low temperature finite size specific heat expression

$$C_v(\beta, L) = \frac{16J^2 \exp(S_1(L) - S_0(L)) \exp(-4J/T)}{L^2 T^2} \quad (1)$$

where $S_1(L)$, $S_0(L)$ are the sample-averaged entropies of the first excited state and the ground state. Setting $J = 1$ a crossover temperature can then be defined by

[5, 14, 15]

$$T^*(L) = 4/(S_1(L) - S_0(L)) \tag{2}$$

which separates the critical behavior in the low temperature ground state dominated regime (with $C_v(\beta, L) \sim \exp(-4/T)/T^2$) and a $T > T^*(L)$ regime where the whole ensemble of higher energy states dominate the thermodynamics [3]. An explicit phenomenological expression for $T^*(L)$ derived from Eq. 5 of Ref. [15], which is consistent with the raw data points [4, 15] for $S_1(L) - S_0(L)$ is

$$\frac{4}{\exp(0.199 \ln(\frac{\ln(6.28L^2)}{2} + L^2(\ln(L^2) - 1)) + 0.473)} \tag{3}$$

A much simpler droplet-based expression from [5] is $T^*(L) \approx L^{-1/2}$. $T^*(L)$ decreases with increasing L because the degeneracy of the excited states increases faster with L than that of the ground state. We will assume [3] that in the $T > T^*(L)$ ThL regime the data can be analysed in the same way as if the energy level distribution were continuous. With this assumption the $T > T^*(L)$ regime will have "effectively continuous" energy level distribution critical exponents with an effective ordering temperature T_c still zero. The ground state dominated regime at $T < T^*(L)$ is a finite size effect which disappears in the infinite L limit.

A non-zero η is to be expected *a priori* for a system with a strong ground state degeneracy, unless each individual ground state is isolated in phase space which is not the case [11] in the bimodal ISG. A droplet analysis of ground state measurements on large sized samples [16] show that $\eta \approx 0.22$, broadly consistent with a number of finite temperature simulation estimates [17–19]. However it has been claimed that in the $T > T^*(L)$ regime the bimodal ISG can be considered to be effectively in the same universality class as the Gaussian ISG [3], meaning that the effective exponents are again $\eta = 0$ and $\nu = 3.50(3)$. In view of the basic definition of η in terms of the short range limit of the spin-spin correlation function $G(r, T) = G[r^{-\eta} \exp(r/\xi(T))]$, this claim is rather surprising.

A major difficulty in establishing the limiting $[T > T^*(L), L \to \infty, T \to 0]$ behavior for ISGs in dimension 2 [14] consists in finding an appropriate and reliable extrapolation procedure from simulation data necessarily restricted in size and in temperature because of the need to achieve good thermal equilibration at large sizes. This is a problem that we will address.

II. SIMULATIONS

The simulations were performed using the Houdayer cluster method [18] in combination with the exchange Monte Carlo [20] method. In the cluster step we first pick a random site i and compute its overlap $q_i = S_i^A S_i^B$, where S_i^A and S_i^B denote the spin for two different replicas. We then build an equal-q cluster along the nearest neighbor interactions and flip all cluster spins in both replicas. We used four replicas which turned out to be remarkably efficacious. On each iteration the replicas are paired at random, then, for each pair, a cluster update is performed, and the usual heat-bath spin update and exchange.

For all systems we used $\beta_{\max} = 3.0$. The number of temperatures were more than 250 for the smallest systems starting at $\beta_{\min} = 0.2$. With increasing system size the number of temperatures was decreased and $\beta_{\min}$ increased. For the largest system (bimodal J_{ij} with $L = 128$) 70 temperatures were used with $\beta_{\min} = 1.2$. The exchange rate was always at least 0.3 for all systems and temperatures. The systems were deemed equilibrated when the average $\langle q^2 \rangle$ for the systems at $\beta_{\max}$ appeared stable between runs. The number of equilibration steps increased with system size, for the bimodal $L = 128$ this took about 600000 steps. After equilibration, at least 200000 measurements were made for each sample for all sizes, taking place after every cluster-sweep-exchange step.

The usual observables were registered, the energy $E(\beta, L)$, the correlation length $\xi(\beta, L)$, the spin overlap moments $\langle |q| \rangle$, $\langle q^2 \rangle$, $\langle |q|^3 \rangle$, $\langle q^4 \rangle$. Correlations $\langle E(\beta, L), U(\beta, L) \rangle$ between the energy and some observables $U(\beta, L)$ were also registered. Thermodynamic derivatives could then be evaluated through the usual $\partial U(\beta, L)/\partial\beta = \langle U(\beta, L), E(\beta, L) \rangle - \langle U(\beta, L) \rangle \langle E(\beta, L) \rangle$. Error estimates of observables and derivatives were done with the bootstrap method.

Sizes studied were $L = 4$, 6, 8, 12, 16, 24, 32, 48, 64, 96, 128 for bimodal interactions, and up to $L = 64$ for the Gaussian interactions, with $2^{13} = 8192$ samples (J_{ij}-interactions) for all sizes.

III. SPECIFIC HEAT

The size dependence of the ground state energy per spin $e(0, L)$ for the 2D Gaussian ISG has been shown [13, 21] to follow the simple critical finite size scaling rule

$$e(0, L) - e(0, \infty) \sim L^{2-\theta} \tag{4}$$

with a θ consistent with the estimate from ground state domain wall stiffness measurements [1]. Standard scaling arguments [4] would suggest that the low temperature specific heat should behave as

$$C_v(\beta, L) \sim \beta^{-2\nu} \approx \beta^{-7} \tag{5}$$

but because of the continuous interaction distribution, in addition to critical excitations there are always single spin excitations. These lead to a term $C_v(\beta, L) \approx T$ which dominates the Gaussian low temperature specific heat as noted by Ref. [4]. Specific heat data for the bimodal model were calculated through the present simulations; data extending to a much lower temperature range

and larger sizes have already been measured using the sophisticated Pfaffian arithmetic technique by Lukic *et al* [4] and by Thomas *et al* [5], and we are very grateful to be able to quote these results *in extenso*.

The data for the two models are shown, see Fig. 1 and Fig. 2, in the form of plots of the derivative $y = \partial \ln(C_v(\beta, L))/\partial\beta$ against $x = T$. This non-conventional form of plot happens to be particularly instructive. A low temperature limit $C_v(\beta, L) \sim T^x$ appears as a straight line through the origin with slope $-x$, while a low temperature limit of the "naïve" bimodal ground state dominated form Eq. (1) appears as a straight line with intercept -4 and slope $+2$.

The Gaussian data are almost independent of L for the whole temperature range. Physically this occurs because the specific heat in ISGs is predominately a near neighbor effect. The curve tends to a slope $\partial y/\partial x \sim -1$ corresponding to $C_v \sim T^1$ in the low T limit, in agreement with the conclusion of Ref. [3].

For the bimodal model there is first a high temperature and/or high L envelope curve corresponding to the effectively continuous $T > T^*(L)$ regime. In this regime finite size effects are very weak : the specific heat is almost independent of L as in the Gaussian. The curves for the two models are of similar form but are not identical. In the large L, low T limit of this envelope curve, the bimodal data as shown in Fig. 2 indicate $C_v \sim T^3$ in agreement with the conclusions drawn in Ref. [5] based on droplet excitation arguments.

For each L the data curve peels off the large L envelope curve below an L-dependent temperature which can be identified with the start of the effectively continuous to ground state dominated regime crossover centered at $T^*(L)$. Finally for each L in the low temperature range $T \ll T^*(L)$ the specific heat links up to the "naïve" limit of Eq. (1). (It should be noted that because of the logarithmic derivative, temperature independent L-dependent factors do not show up in this plot). The crossover can be seen to be gentle for small L, becoming sharp for large L. Defining $T^*(L)$ as the location of the maximum positive slope on this plot, the crossover temperatures can be clearly identified and are consistent with $T^*(L)L^{1/2} = 1.1(1)$.

An anomalous limit of the form

$$C_v(\beta) \sim \beta^2 \exp(-2\beta) \tag{6}$$

which has been proposed by some authors [4, 22] following Ref. [23] is inconsistent with the data in Fig. 2 for all L and T (see also [24, 25]). An intermediate L regime where $C_v(\beta, L) \sim T^{5.25}$ as proposed in Ref. [15] or $C_v(\beta, L) \sim T^{4.2}$ as proposed in Ref. [14] appear to be valid only for a limited range of T and L.

IV. THE EXPONENT η

For ISGs with non-zero critical temperatures finite size scaling analyses at and close to the critical temperature are used to estimate critical exponents. For the 2D bimodal ISG, because of the crossover to the ground state dominated regime this approach is ruled out and the critical exponents must be estimated using the entirely different strategy of ThL measurements.

The standard Renormalization Group theory (RGT) scaling variable for models with non-zero ordering temperatures is $t = (T - T_c)/T_c$. This obviously cannot be used when $T_c = 0$; by convention the scaling variable used in the literature for 2D ISGs is the un-normalized temperature T. This is only a convention; it is perfectly legitimate to use other conventions. Thus, when considering the canonical 1D Ising ferromagnet, Baxter [26] remarks "When $T_c = 0$ it is more sensible to replace $t = (T - T_c)/T_c$ by $\tau = \exp(-2\beta)$". (In fact for the particular 1D model scaling without corrections over the entire temperature range follows if a related scaling variable $\tau = 1 - \tanh(\beta)$ is chosen [27, 28]). Below we will introduce another scaling variable appropriate for ISGs with $T_c = 0$, but for the moment we follow this traditional $t = T$ 2D ISG convention. The critical exponents are defined through the leading ThL expressions for the reduced susceptibility and the second moment correlation length within this convention : $\chi(T) = C_\chi T^{-(2-\eta)\nu}$ and $\xi(T) = C_\xi T^{-\nu}$ in the limit $T \to 0, L \to \infty$. For all data which fulfil the condition (either in the bimodal and Gaussian models) $L > K\xi(T, L)$ with $K \approx 6$, observables such as $\chi(T, L)$ and $\xi(T, L)$ depend on T but not on L, and so correspond to the ThL infinite size values $\chi(T)$ and $\xi(T)$. The ThL condition defines implicitly a crossover temperature $T_\xi(L)$. It turns out that in the bimodal 2D ISG the ThL limit temperature $T_\xi(L)$ is always higher than the corresponding crossover temperature to the ground state dominated regime $T^*(L)$ defined above, so the ThL data are always well in the effectively continuous regime. The ThL data extrapolation to $T = 0$ corresponds to estimates for the critical exponents in the successive limits $[L \to \infty, T \to 0]$ so in the effectively continuous energy level regime, to be distinguished from the exponents defined taking the successive limits $[T \to 0, L \to \infty]$ which would correspond to the "finite size" ground state dominated regime.

There have been many previous studies having the aim of estimating the critical exponents and in particular η for the bimodal model. McMillan already in 1983 estimated $\eta = 0.28(4)$ from $G(r)$ correlation data on one $L = 96$ sample well in the effectively continuous regime [17]. Katzgraber and Lee [19] estimated $\eta = 0.138(5)$ from $\chi(T, L)$ data. Jörg *et al* [3] show a plot of $\ln \chi(T)$ against $\ln \xi(T)$ after an extrapolation to infinite L using the technique of Ref. [29]. They state "fits of this curve lead to values of η that are very small, between 0 and 0.1, strongly suggestive of $\eta = 0$". However, this type of extrapolation to infinite L is delicate, particularly in the bimodal 2D case.

In addition, the data displayed by [3] on a $\ln \chi(T) - \ln \xi(T)$ plot extending over five decades on the y axis are hard to fit with precision. Katzgraber *et al* [14]

show a plot of $\partial \ln \chi(T,L)/\partial \ln \xi(T,L)$ which in principle is equivalent to the Ref. [3] plot but which provides a display much more sensitive to the value of η; they state cautiously "for all system sizes and temperatures studied $\eta_{\rm eff}$ is always greater than 0.2, although an extrapolation to $\eta = 0$ cannot be ruled out", so that the possibility of the bimodal and Gaussian ISGs being in the same universality class "cannot be reliably proven". In Refs. [32, 33] it is claimed that the Gaussian and bimodal models are in the same universality class, which is surprising as "the data are not sufficiently precise to provide a precise determination of η, being consistent with a small value $\eta \leq 0.2$, including $\eta = 0$".

All the estimates quoted so far can be considered to concern the effectively continuous regime. At zero or low temperatures, so in the ground state dominated regime, different sophisticated algorithms lead to the estimates $\eta = 0.14(1)$ [12], and to $\eta = 0.22$ [16].

In Fig. 3 and Fig. 4, we show plots of $y = \partial \ln \chi(T,L)/\partial \ln \xi(T,L)$ against $x = 1/\xi(T,L)$ for the Gaussian and bimodal models. These are *raw* data points having the high statistical precision of the present measurements. With the conventional definition of the critical exponents through $\chi(T,L) \sim T^{(2\eta)\nu}$ and $\xi(T,L) \sim T^{\nu}$ in the ThL regime low-T limit, the limiting slope $\partial y/\partial x$ at criticality as $x \to 0$ is by definition equal to $2-\eta$. For the Gaussian model the observed tendency of the slope is consistent with the limit of $\eta = 0$ which must be the case for this nondegenerate ground state model. For the bimodal model the observed $y(x)$ in the ThL regime is not tending to 2 but to a constant limit of 1.80(2). Slight overshoots for each L in both systems can be ascribed to $\chi(T,L)$ and $\xi(T,L)$ not reaching the ThL condition at quite the same temperature. As stated above, very similar observations were made in Ref. [14] for the bimodal model. The present results thus confirm unambiguously that for the bimodal ISG in the effectively continuous regime η is not zero but is ≈ 0.20. Thus the bimodal ISG in the effectively continuous ThL regime and the Gaussian ISG are not in the same universality class.

It has been shown that in dimension 4 also, Gaussian and bimodal ISGs are not in the same universality class [34], so the breakdown of universality in ISGs appears to be general.

V. SCALING AND ZERO TEMPERATURE ORDERING

Estimating the exponents ν or $\gamma = (2-\eta)\nu$ is more difficult than for the exponent η. As we have noted above, the standard RGT convention for models with finite temperature ordering is to use the scaling variable $t = (T/T_c) - 1$, which obviously cannot be applied to models with $T_c = 0$, and for 2D ISGs the preferred convention in the literature has been to use the un-normalized scaling variable $t = T$. In practice this is inefficient as the extrapolations towards the $T = 0$ limit in order to estimate the values for the critical exponents are very ambiguous. For instance, when presenting T-scaled susceptibility data for sizes up to $L = 128$ Katzgraber *et al* [14] state "the [susceptibility] data for the bimodal case can be extrapolated to any arbitrary value including $1/\gamma_{\rm eff} = 0$".

We will introduce a novel scaling variable suitable for the 2D ISGs, applying the same principles as for ISGs at higher dimensions [6], adapted to $T = 0$ ordering :

– For spin glasses the relevant interaction strength parameter is not J but is $\langle J^2 \rangle$, so the natural dimensionless parameter is $\langle J^2 \rangle \beta^2$ (or alternatively $\tanh^2(J\beta)$ for bimodal ISGs). With the standard normalisation $\langle J^2 \rangle = 1$ the natural inverse "temperature" in ISGs is β^2, not β. This was recognized immediately after the Edwards-Anderson model was introduced, in high temperature series expansion (HTSE) analyses for ISGs including 2D models [35–37], but has since been overlooked in most simulation analyses.

– It is convenient to choose a scaling variable τ defined in such a way that $\tau = 0$ at criticality and $\tau = 1$ at infinite temperature. With an ISG ordering at a finite inverse temperature β_c, $\tau(\beta) = 1 - \beta^2/\beta_c^2$ is an appropriate choice [6, 37]. When $\beta_c = \infty$ as in the 2D ISG case, $\tau_t(\beta) = 1 - (\tanh(\beta)/\tanh(\beta_c))^2 = 1 - \tanh(\beta)^2$ has been used [35], but here we will prefer $\tau_b(\beta) = 1/(1+\beta^2)$ as it turns out to be efficient and the limits are easy to relate to those of the T scaling convention. With non-zero T_c the effective exponents at criticality do not depend on the choice of scaling variable; this is not the case when $T_c = 0$, but a simple dictionary is given below relating the limiting derivatives for τ_b scaling to the exponents for the conventional T scaling.

– The ThL HTSE Darboux [38] format for observables $Q(x)$ is

$$Q(x) = 1 + a_1 x + a_2 x^2 + a_3 x^3 + \cdots \qquad (7)$$

with $x = \beta^2$ in ISGs [37]. The HTSE ISG susceptibility $\chi(\beta^2)$ is naturally in this format, so for ISG models with $T_c > 0$ the ThL susceptibility can be scaled in the Wegner [39] form

$$\chi(\beta^2) = C_\chi \tau(\beta^2)^{-(2-\eta)\nu} F[1 + a_\chi \tau(\beta^2)^\theta + \cdots] \qquad (8)$$

Because the correlation function second moment μ_2 HTSE is of the form (see Ref. [40] for the Ising ferromagnet)

$$\mu_2(x) = x + a_1 x^2 + a_2 x^3 + \cdots \qquad (9)$$

and the second moment correlation length is defined through $\xi(x)^2 = \mu_2/(z\chi(x))$ with z the number of nearest neighbors, for consistency the appropriate correlation length variable for ISG scaling is $\xi(x)/\beta$ rather than $\xi(x)$ (whether T_c is zero or not). This point has been spelt out in Ref. [6].

Examples of applications of the scaling rules outlined here to other specific models (both ferromagnets and

ISGs) have been given elsewhere. A general discussion of ferromagnets and spin glasses is given in Ref. [6], analyses of 3D Ising, XY and Heisenberg ferromagnets in Ref. [41], the 2D Ising ferromagnet is analysed in Ref. [42], 3D Ising ferromagnets in [28, 43], high dimension Ising ferromagnets in Ref. [44], and the 2D Villain fully frustrated model in Ref. [27].

The scaling of the Binder cumulant

$$g(\beta^2) = \frac{1}{2}\left(3 - \frac{[\langle q^4 \rangle]}{[\langle q^2 \rangle]^2}\right) \tag{10}$$

is discussed in the Appendix. The 2D simulation data analysis and the extrapolations below are based on the derivatives $\partial \ln Q(\tau_b, L)/\partial \ln \tau_b$ in the ThL regime where these derivatives are independent of L and so equal to the infinite size derivatives. An advantage of the 2D models is that in contrast to $\tau(\beta^2)$ for the models with non-zero T_c, for the 2D ISGs with $T_c \equiv 0$ there is no uncertainty in the definition of $\tau_b(\beta^2)$ related to an uncertainty in the value of the ordering temperature.

Once the $\tau_b \to 0$ limits for the various derivatives have been estimated by extrapolation of the ThL data for finite L, there is a simple dictionary for translating into terms of the conventional T scaling critical exponents ν and η defined above :

$$-\frac{\partial \ln \chi(\tau_b)}{\partial \ln \tau_b} \to \frac{\nu(2-\eta)}{2} \tag{11a}$$

$$-\frac{\partial \ln(T\xi(\tau_b))}{\partial \ln \tau_b} \to \frac{(\nu-1)}{2} \tag{11b}$$

$$\frac{\partial \ln \chi(\tau_b)}{\partial \ln(T\xi(\tau_b))} \to \frac{\nu(2-\eta)}{\nu-1} \tag{11c}$$

$$-\frac{\partial \ln g(\tau_b)}{\partial \ln \tau_b} \to \nu \tag{11d}$$

VI. ANALYSES WITH THE SCALING VARIABLE τ_b

The four derivatives of Eq. (11) are shown in Figs. 5 to 12. In contrast to the derivatives in which T is used as the scaling variable, each derivative can be extrapolated in a fairly unambiguous manner to criticality, and always has an exact finite value at infinite temperature $\tau_b = 1$.

The exact infinite temperature limits from the general high temperature scaling expansion expressions [37] applied to scaling with τ_b are (when $\tau_b \to 1$):

$$-\frac{\partial \ln \chi(\tau_b)}{\partial \ln \tau_b} = 4\,(\text{Gauss.}), \ldots = 4\,(\text{bimodal}) \tag{12a}$$

$$\frac{\partial \ln(T\xi(\tau_b))}{\partial \ln \tau_b} = 1\,(\text{Gauss.}), \ldots = \frac{5}{3}\,(\text{bimodal}) \tag{12b}$$

$$\frac{\partial \ln \chi(\tau_b)}{\partial \ln(T\xi(\tau_b))} = 4\,(\text{Gauss.}), \ldots = \frac{12}{5}\,(\text{bimodal}) \tag{12c}$$

The extrapolation method is outlined in Appendix II. With $\eta = 0$ and assuming $\nu = 3.48(5)$ [11], the predicted Gaussian critical limits (when $\tau_b \to 0$) for the derivatives are

$$-\frac{\partial \ln \chi(\tau_b)}{\partial \ln \tau_b} \to 3.48(5) \tag{13a}$$

$$-\frac{\partial \ln(T\xi(\tau_b))}{\partial \ln \tau_b} \to 1.24(3) \tag{13b}$$

$$\frac{\partial \ln \chi(\tau_b)}{\partial \ln(T\xi(\tau_b))} \to 2.81(1) \tag{13c}$$

$$-\frac{\partial \ln g(\tau_b)}{\partial \ln \tau_b} \to 3.5(3) \tag{13d}$$

From the fitted ThL data extrapolations (see Appendix II) the estimated Gaussian critical limit values are 3.40(10), 1.25(5), 2.90(10), 3.6(1) respectively. These values are fully consistent with the list above, validating the approach and the extrapolation procedure that we have used. For the bimodal data, the extrapolated ThL limits (when $\tau_b \to 0$) from the figures (see Appendix II) give estimates

$$-\frac{\partial \ln \chi(\tau_b)}{\partial \ln \tau_b} \to 4.3(1) \tag{14a}$$

$$-\frac{\partial \ln(T\xi(\tau_b))}{\partial \ln \tau_b} \to 1.9(1) \tag{14b}$$

$$\frac{\partial \ln \chi(\tau_b)}{\partial \ln(T\xi(\tau_b))} \to 2.15(10) \tag{14c}$$

$$-\frac{\partial \ln g(\tau_b)}{\partial \ln \tau_b} \to 4.7(1) \tag{14d}$$

These are all significantly different from the Gaussian values, confirming non-universality. When translated into the T scaling convention, the 2D bimodal critical exponents from these measurements are $\eta = 0.20(2)$ and $\nu = 4.8(2)$ (so $\gamma = (2-\eta)\nu = 8.6(4)$). Not only is the ThL bimodal exponent η different from the Gaussian value but the ν value is different also.

VII. CONCLUSION

Simulation data are presented for the Gaussian and bimodal interaction distribution Ising spin glasses in dimension two, which are known to order only at zero temperature. In order to facilitate extrapolations to zero temperature, a temperature scaling variable $\tau_b = T^2/(1+T^2)$ is introduced in addition to the traditional 2D ISG scaling variable $t = T$. The Gaussian simulation data are completely consistent with the well established critical behavior for this model, with exponents $\eta \equiv 0$ and $\nu = 3.48(5)$ [11].

The bimodal specific heat simulation data supplemented by data from Lukic *et al* [4] and from Thomas *et al* [5] show clear crossovers from an effectively continuous energy level thermodynamic limit regime to a finite size ground state dominated regime at size dependent temperatures $T^*(L) \approx 1.1/L^{1/2}$ (see Ref. [5]).

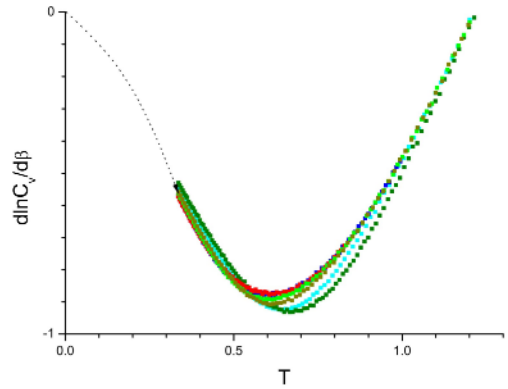

FIG. 1. (Color on line) Gaussian 2D ISG. Logarithmic derivative of the specific heat $\partial \ln C_v(T,L)/\partial\beta$ against T. Sizes $L = 64$, 48, 32, 24, 16, 12 top to bottom in the dip. Curve : extrapolation.

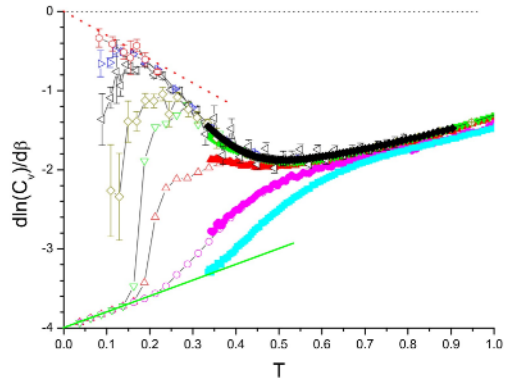

FIG. 2. (Color on line) Bimodal 2D ISG. Logarithmic derivative of the specific heat $\partial \ln C_v(T,L)/\partial\beta$ against T. Full points : simulation data $L = 96$, 48, 24, 12, 8 (black, green, red, pink, cyan) top to bottom. Open points : Pfaffian data ; red polygons $L = 512$, blue right triangles $L = 256$, black left triangles $L = 128$, brown diamonds $L = 64$ (all data from Ref. [5]), green down triangles $L = 50$, red up triangles $L = 24$, pink circles $L = 12$, all data fom Ref. [4]. Dashed diagonal red line $y = -3x$, green diagonal line $y = -4 + 2x$.

The extrapolated ThL simulation results tend to critical limits which correspond consistently to $\eta = 0.20(2)$ and $\nu = 4.8(2)$, clearly different from the Gaussian values. This demonstrates that the standard universality rules do not hold for 2D ISG models. In dimension 4 also bimodal and Gaussian ISGs have been shown not to be in the same universality class either [34], strongly suggesting a lack of universality for ISGs in each dimension (presumably up to the upper critical dimension).

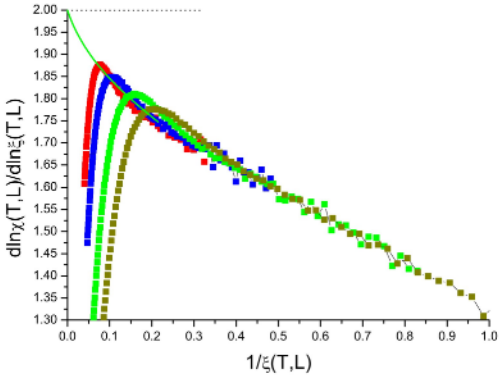

FIG. 3. (Color on line) Gaussian 2D ISG. Derivative $\partial \ln \chi(T,L)/\partial \ln \xi(T,L)$ against $1/\xi(T,L)$ for $L = 64$, 48, 32, 24 left to right. In this and all following figures both Gaussian and bimodal, the color coding is : black, pink, red, blue, green, brown, cyan, olive for $L = 128$, 96, 64, 48, 32, 24, 16, 12.

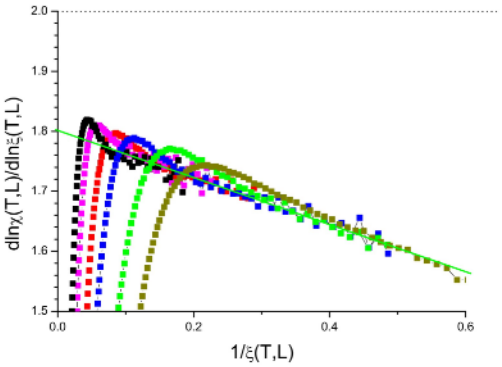

FIG. 4. (Color on line) Bimodal 2D ISG. Derivative $\partial \ln \chi(T,L)/\partial \ln \xi(T,L)$ against $1/\xi(T,L)$ for $L = 128$, 96, 64, 48, 32, 24 left to right. Same color coding as in Fig. 3.

VIII. APPENDIX I: BINDER CUMULANT

The ferromagnetic Binder cumulant has been extensively exploited in the FSS limit regime very close to criticality for its properties as a dimensionless observable. In addition its ThL properties can also be studied. In Ising ferromagnets, the critical exponent for the second field derivative of the susceptibility χ_4 (also called the non-linear susceptibility), is [40]

$$\gamma_4 = \gamma + 2\Delta = \nu d + 2\gamma \tag{15}$$

The non-linear susceptibility χ_4 is directly related to the Binder cumulant, [45] Eq. 10.2, through

$$g(\beta, L) = \frac{-\chi_4}{L^d \chi^2} = \frac{3\langle m^2\rangle - \langle m^4\rangle}{\langle m^2\rangle^2} \tag{16}$$

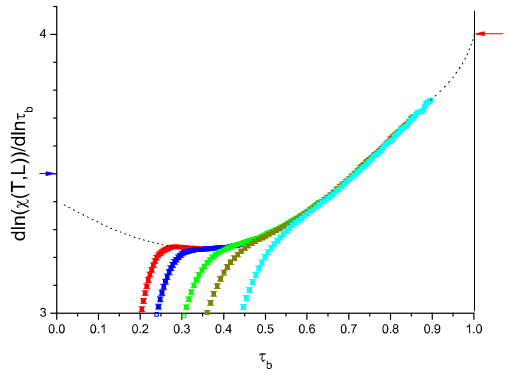

FIG. 5. (Color on line) Gaussian 2D ISG. The derivative $\partial \ln \chi(T,L)/\partial \ln \tau_b$ against τ_b. Sizes $L = 64$, 48, 32, 24, 16 left to right. Same color coding as in Fig. 3. Dashed line: extrapolation. Red arrow : exact infinite temperature value. Blue arrow : Gaussian critical value.

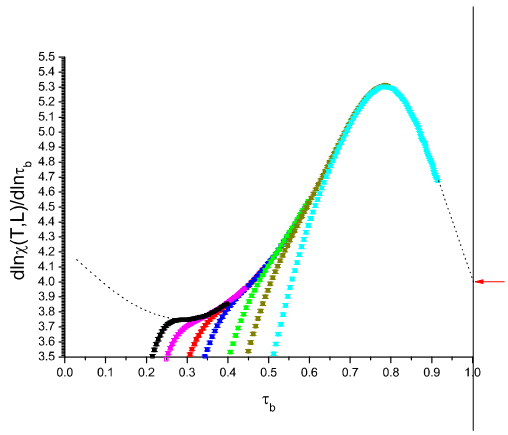

FIG. 6. (Color on line) Bimodal 2D ISG. The derivative $\partial \ln \chi(T,L)/\partial \ln \tau_b$ against τ_b. Sizes $L = 128$, 96, 64, 48, 32, 24, 16 left to right. Same color coding as in Fig. 3. Dashed line: extrapolation. Red arrow : exact infinite temperature value.

As χ scales with the critical exponent γ, the normalized Binder cumulant $L^d g(\beta, L)$ scales with the ThL regime critical exponent $\partial \ln(L^d g)/\partial \ln \tau = (\nu d + 2\gamma) - 2\gamma = \nu d$. In any $S = 1/2$ Ising system the infinite temperature (independent spin) limit for the Binder cumulant is

$$g(\infty, N) \equiv 1/N \tag{17}$$

where N is the number of spins; $N = L^d$ for a hypercubic lattice. So $L^d g(\beta, L)$ has an infinite temperature limit which is strictly 1, and a large L critical limit (with corrections as for the other observables):

$$L^d g(\tau_b, L) \sim \tau_b^{-\nu d}\,(1 + \cdots) \tag{18}$$

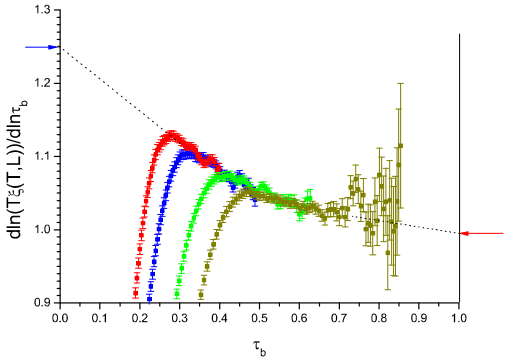

FIG. 7. (Color on line) Gaussian 2D ISG. The derivative $\partial \ln(T\xi(T,L))/\partial \ln \tau_b$ against τ_b. Sizes $L = 64$, 48, 32, 24 left to right. Same color coding as in Fig. 3. Dashed line: extrapolation. Red arrow : exact infinite temperature value. Blue arrow : Gaussian critical value.

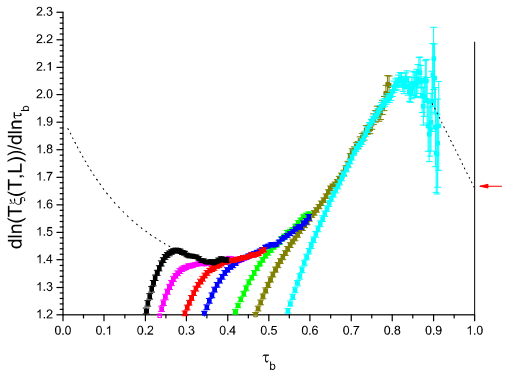

FIG. 8. (Color on line) Bimodal 2D ISG. The derivative $\partial \ln(T\xi(T,L))/\partial \ln \tau_b$ against τ_b. Sizes $L = 128$, 96, 64, 48, 32, 24, 16 left to right. Same color coding as in Fig. 3. Dashed line: extrapolation. Red arrow : exact infinite temperature value.

Exactly the same argument can be transposed to ISGs (see Ref. [36] for χ_4 in ISGs). In the particular case of a 2D ISG model with τ_b scaling, the critical value for the derivative $\partial \ln(L^d g(\tau_b, L))/\partial \ln \tau_b$ of the Binder cumulant ThL data extrapolated to $\tau_b = 0$ is $2\nu/2 = \nu$ where ν is once again the correlation length critical exponent in the T scaling convention. The Binder cumulant data plotted in the Eq. (18) form are shown for the two models in Figs. 13 and 14. The ThL envelope curves can be seen by inspection. The derivatives of these curves have already been shown in Figs. 9 and 10.

It has been suggested that if two models have the same function when $y = g(\beta, L)$ is plotted against $x = \xi(\beta, L)/L$, it is a proof of universality. However, because both $Lg^{1/d}(\beta, L)$ and $\xi(\beta, L)$ are controlled by just the same exponent ν this is questionable.

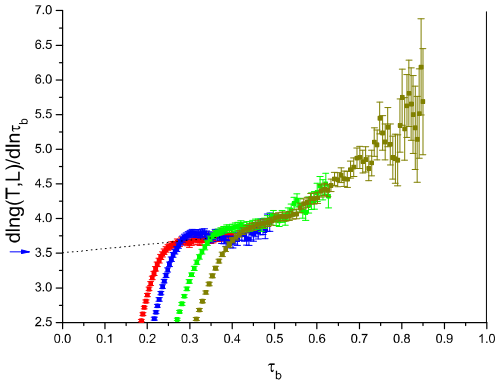

FIG. 9. (Color on line) Gaussian 2D ISG. The derivative $\partial \ln g(T,L)/\partial \ln \tau_b$ against τ_b, where $g(T,L)$ is the Binder cumulant. $L = 64$, 48, 32, 24 left to right. Same color coding as in Fig. 3. Line: extrapolation. Blue arrow : Gaussian critical value.

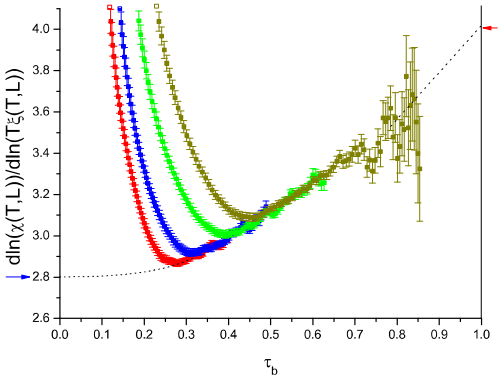

FIG. 11. (Color on line) Gaussian 2D ISG. The derivative $\partial \ln \chi(T,L)/\partial \ln(T\xi(T,L))$ against τ_b. Sizes $L = 64$, 48, 32, 24 left to right. Same color coding as in Fig. 3. Dashed line: extrapolation. Red arrow : exact infinite temperature value. Blue arrow : Gaussian critical value.

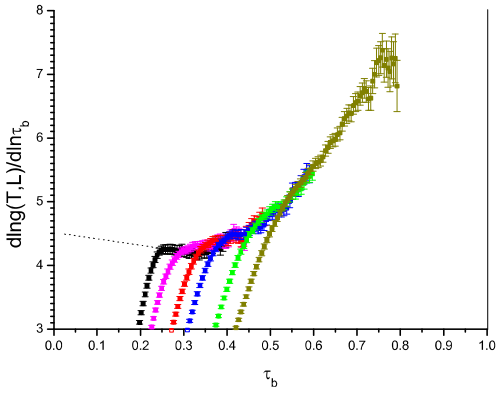

FIG. 10. (Color on line) Bimodal 2D ISG. The derivative $\partial \ln g(T,L)/\partial \ln \tau_b$ against τ_b, where $g(T,L)$ is the Binder cumulant. Sizes $L = 128$, 96, 64, 48, 32, 24 left to right. Same color coding as in Fig. 3. Line: extrapolation.

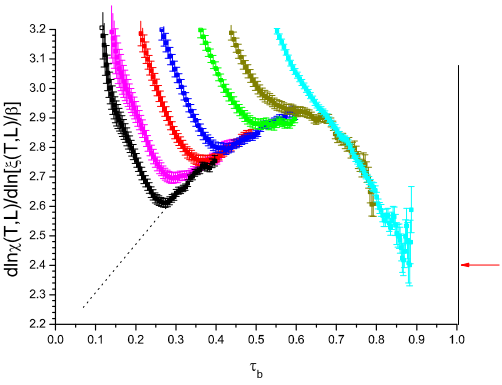

FIG. 12. (Color on line) Bimodal 2D ISG. The derivative $\partial \ln \chi(T,L)/\partial \ln(T\xi(T,L))$ against τ_b. Sizes $L = 128$, 96, 64, 48, 32, 24, 16 left to right. Same color coding as in Fig. 3. Dashed line: extrapolation. Red arrow : exact infinite temperature value.

IX. APPENDIX II

As the data sets do not extend to infinite size, to estimate the critical $\tau_b = 0$ limit values from the ThL derivative data in Figs. 5 to 12, an extrapolation must be made. There is no definitive method to extrapolate so as to be sure to obtain exact values of the critical exponents, though data to still larger sizes would make the task easier. The most economical choice for extrapolation is to assume that the ThL derivative data continue to evolve smoothly and regularly when an extrapolation is made towards $\tau_b = 0$ through the smaller τ_b region where no ThL data are for the moment available. To do this, for each derivative observable $y(x)$ with $x = \tau_b$ we collect together the ThL data points for all the sizes L up to $x = 0.6$ and make standard polynomial fits with 3 or 4 terms $y(x) = a_0 + a_1 x + a_2 x^2$ or $y(x) = a_0 + a_1 x + a_2 x^2 + a_3 x^3$ (in fits with larger numbers of terms the fit parameter values become unstable). Assuming that each polynomial fit curve extended to $\tau_b = 0$ is a good approximation to the true behavior, each a_0 is an estimate for the critical limit value. The a_0 values for 3 or 4 parameter fits turn out to be similar. In Figs. 15, 16, 17 and 18 the data and fits are shown for $\partial \ln \chi(\tau_b)/\partial \ln \tau_b$, $\partial \ln(T\xi(\tau_b))/\partial \tau_b$ and $\partial \ln \chi(\tau_b)/\partial \ln(T\xi(\tau_b))$ and $\partial \ln g(\tau_b)/\partial \ln \tau_b$ for both Gaussian and bimodal models. The fits are automatic, so this procedure is objective and we assume that it is optimal for the available data. All the Gaussian extrap-

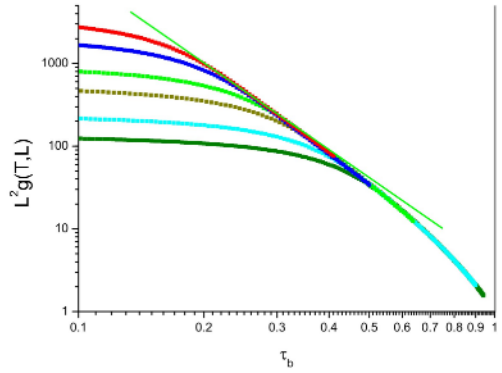

FIG. 13. (Color on line) Gaussian 2D ISG. $L^2 g(\tau_b)$ against τ_b. Sizes $L = 64$, 48, 32, 24, 16, 12 top to bottom. Same color coding as in Fig. 3. $g(T, L)$ is the Binder cumulant. Line slope -3.5.

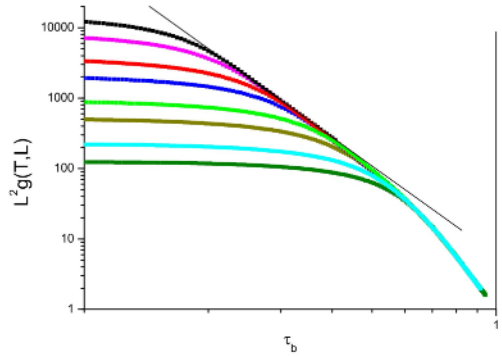

FIG. 14. (Color on line) Bimodal 2D ISG. $L^2 g(\tau_b)$ against τ_b. Sizes $L = 128$, 96, 64, 48, 32, 24, 16, 12 top to bottom. Same color coding as in Fig. 3. $g(T, L)$ is the Binder cumulant. Line slope -4.2.

olated critical values estimated in this way are close to those expected assuming the published exponents, $\eta = 0$ and $\nu = 3.48(5)$ [11]. This implies that the estimated bimodal critical values are also close to the true critical limits.

ACKNOWLEDGMENTS

We are very grateful to Olivier Martin and to Alan Middleton who generously allow us access to the specific heat data of Ref. [4] and of Ref. [5] respectively. We would like to thank Alex Hartmann for very helpful suggestions. The computations were performed on resources provided by the Swedish National Infrastructure for Computing (SNIC) at the High Performance Computing Center North (HPC2N) and Chalmers Centre for Computational Science and Engineering (C3SE).

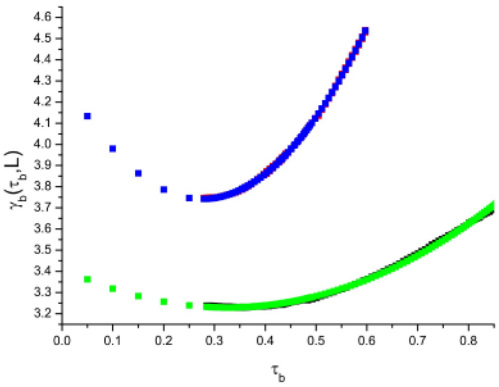

FIG. 15. (Color on line) The ThL $\partial \ln \chi(\tau_b)/\partial \ln \tau_b$ data for the Gaussian model from Fig. 5, (lower, black) with the polynomial fit (green), and for the bimodal model from Fig. 6, (upper, red) with the polynomial fit (blue).

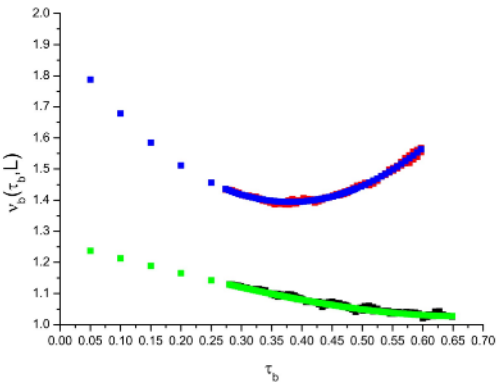

FIG. 16. (Color on line) The ThL $\partial \ln(T\xi(\tau_b)/\partial \tau_b$ data for the Gaussian model from Fig. 7, (lower, black) with the polynomial fit (green), and for the bimodal model from Fig. 8, (upper, red) with the polynomial fit (blue).

[1] A. K. Hartmann and A. P. Young, Phys. Rev. B **64**, 18404 (2001).

[2] M. Ohzeki and H. Nishimori, J. Phys. A: Math. Theor. **42**, 332001 (2009).

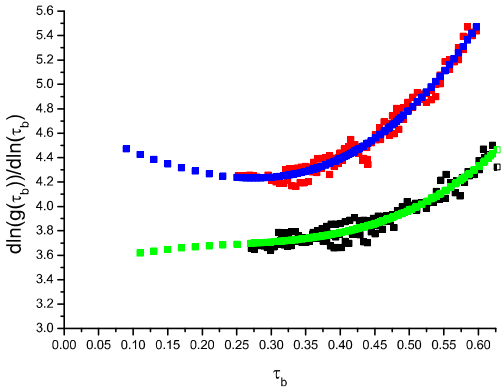

FIG. 17. (Color on line) The ThL $\partial \ln g(\tau_b)/\partial \ln(\tau_b)$ data for the Gaussian model from Fig. 9, (lower, black) with the polynomial fit (green), and for the bimodal model from Fig. 10, (upper, red) with the polynomial fit (blue).

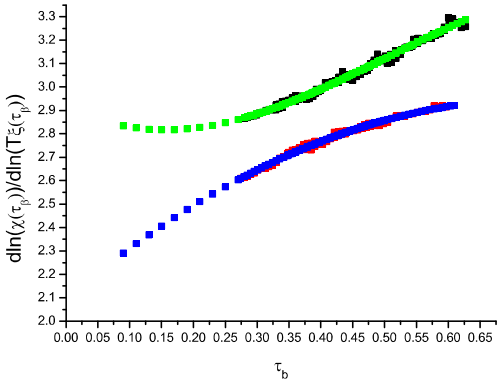

FIG. 18. (Color on line) The ThL $\partial \ln \chi(\tau_b)/\partial \ln(T\xi(\tau_b))$ data for the Gaussian model from Fig. 11, (upper, black) with the polynomial fit (green), and for the bimodal model from Fig. 12, (lower, red) with the polynomial fit (blue).

[3] T. Jörg, J. Lukic, E. Marinari, O. C. Martin, Phys. Rev. Lett. **96**, 237205 (2006).
[4] J. Lukic, A. Galluccio, E. Marinari, O. C. Martin and G. Rinaldi, Phys. Rev. Lett. **92**, 117202 (2004).
[5] C. K. Thomas, D. A. Huse, and A. A. Middleton, Phys. Rev. Lett. **107**, 047203 (2011).
[6] I. A. Campbell, K. Hukushima, and H. Takayama, Phys. Rev. Lett. **97**, 117202 (2006).
[7] H. Rieger, L. Santen, U. Blasum, M. Diehl, M. Jünger, and G. Rinaldi, J. Phys. A **29**, 3939 (1996); **30**, 8795(E) (1997).
[8] A. C. Carter, A. J. Bray, and M. A. Moore, Phys. Rev. Lett. **88**, 077201 (2002).
[9] C. Amoruso, E. Marinari, O. C. Martin, and A. Pagnani, Phys. Rev. Lett. **91**, 087201 (2003).
[10] J. Houdayer and A. K. Hartmann, Phys. Rev. B **70**, 014418 (2004).
[11] A. K. Hartmann, A. J. Bray, A. C. Carter, M. A. Moore, and A. P. Young, Phys. Rev. B **66**, 224401 (2002)
[12] J. Poulter and J. A. Blackman, Phys. Rev. B **72**, 104422 (2005).
[13] K. T. Creighton and A. A. Middleton Phys. Rev. B **77**, 144418 (2008).
[14] H. G. Katzgraber, Lik Wee Lee, and I. A. Campbell, Phys. Rev. B **75**, 014412 (2007).
[15] R. Fisch, J. Stat. Phys. **128**, 1113 (2007).
[16] A. K. Hartmann, Phys. Rev. B **77**, 144418 (2008).
[17] W. L. McMillan, Phys. Rev. B **28**, 5216 (1983).
[18] J. Houdayer, Eur. Phys. J. B **22**, 479 (2001).
[19] H. G. Katzgraber and Lik Wee Lee, Phys. Rev. B **71**, 134404 (2005).
[20] K. Hukushima and K. Nemoto, J. Phys. Soc. Japan **65**, 1604 (1996).
[21] I. A. Campbell, A. K. Hartmann and H. G. Katzgraber, Phys. Rev. B **70** 054429 (2004).
[22] J.-S. Wang, Phys. Rev. E **72**, 036706 (2005).
[23] J.-S. Wang and R. H. Swendsen, Phys. Rev. B **38**, 4840 (1988).
[24] L. Saul and M. Kardar, Phys. Rev. E **48**, R3221 (1993).
[25] W. Atisattapong and J. Poulter, New Journal of Physics **10** 09312 (2008).
[26] R. J. Baxter "Exactly solved models in Statistical Mechanics" Academic Press (London) (1982).
[27] H. G. Katzgraber, I. A. Campbell, and A. K. Hartmann, Phys. Rev. B **78**, 184409 (2008).
[28] I. A. Campbell and P. H. Lundow, Phys. Rev. B **83**, 014411 (2011).
[29] S. Caracciolo *et al.*, Phys. Rev. Lett. **74**, 2969 (1995).
[30] M. Palassini and S. Caracciolo, Phys. Rev. Lett. **82**, 5128 (1999).
[31] M. Baity-Jesi *et al.*, Phys. Rev. B **88**, 224416 (2013).
[32] F. Parisen Toldin, A. Pelissetto, and E. Vicari, Phys. Rev. E **82**, 021106 (2010).
[33] F. Parisen Toldin, A. Pelissetto, and E. Vicari, Phys. Rev. E **84**, 051116 (2011).
[34] P. H. Lundow and I. A. Campbell, Phys. Rev. E **91**, 042121 (2015), Physica A **434**, 181 (2015).
[35] R. R. P. Singh and S. Chakraverty, Phys. Rev. B **36**, 559 (1987).
[36] L. Klein, J. Adler, A. Aharony, A. B. Harris and Y. Meir, Phys. Rev. B **43**, 11249 (1991).
[37] D. Daboul, I. Chang, and A. Aharony, Eur. Phys. J. B **41**, 231 (2004).
[38] J. G. Darboux, J. Math. Pures Appl. **4**, 377 (1878).
[39] F. J. Wegner, Phys. Rev. B **5**, 4529 (1972).
[40] P. Butera and M. Comi, Phys. Rev. B **65**, 144431 (2002).
[41] I. A. Campbell, K. Hukushima, and H. Takayama, Phys. Rev. B **76**, 134421 (2007).
[42] I. A. Campbell and P. Butera, Phys. Rev. B **78**, 024435 (2008).
[43] P. H. Lundow and I. A. Campbell, Phys. Rev. B **83**, 184408 (2011).
[44] B. Berche, C. Chatelain, C. Dhall, R. Kenna, R. Low, and J. C. Walter, J. Stat. Mech. P11010 (2008).
[45] V. Privman, P. C. Hohenberg and A. Aharony, "Universal Critical-Point Amplitude Relations", in "Phase Transitions and Critical Phenomena" (Academic, NY, 1991), eds. C. Domb and J.L. Lebowitz, **14**, 1.